



Contents lists available at ScienceDirect

Applied Clay Science

journal homepage: [www.elsevier.com/locate/clay](http://www.elsevier.com/locate/clay)

Research paper

# Stearic acid modified montmorillonite as emerging microcapsules for thermal energy storage

Kang Peng<sup>a</sup>, Liangjie Fu<sup>a,\*</sup>, Xiaoyu Li<sup>a</sup>, Jing Ouyang<sup>a,b</sup>, Huaming Yang<sup>a,b,c,\*\*</sup><sup>a</sup> Centre for Mineral Materials, School of Minerals Processing and Bioengineering, Central South University, Changsha 410083, China<sup>b</sup> Hunan Key Lab of Mineral Materials and Application, Central South University, Changsha 410083, China<sup>c</sup> State Key Lab of Powder Metallurgy, Central South University, Changsha 410083, China

## ARTICLE INFO

## Article history:

Received 10 March 2016

Received in revised form 15 December 2016

Accepted 3 January 2017

Available online xxxxx

## Keywords:

Montmorillonite

Microcapsules

Phase change materials

Self-assembly

Thermal energy storage

## ABSTRACT

In order to obtain an efficient phase change material (PCM), emerging montmorillonite/stearic acid (Mt/SA) microcapsules containing SA core with Mt shell were designed and prepared via self-assembly of Mt in the SA emulsion. The Mt/SA microcapsules were coated with SiO<sub>2</sub> from the hydrolysis and polycondensation of TEOS to enhance the structure stability. The microstructure, thermal properties and reliability of Mt/SA microcapsules were investigated via scanning electron microscopy (SEM) and differential scanning calorimetry (DSC). The Mt/SA microcapsules presented sphere-like particles and had a size distribution from 10 to 30 μm. The freezing latent heat of the Mt/SA microcapsules was 118 J/g at 52.3 °C. The energy storage rate of the Mt/SA microcapsules was faster compared to SA. The Mt/SA microcapsules had excellent structural stability, high energy storage capacity and stable energy storage and release performances. The energy storage performances of the Mt/SA microcapsules were superior to the Mt/SA composites prepared via vacuum impregnation. Excellent energy storage reliability and capability of the Mt/SA microcapsules have advantages for solar energy storage fields.

© 2017 Published by Elsevier B.V.

## 1. Introduction

Over the past few decades, the growing consumption of fossil fuels has brought about a heavy energy crisis and environmental pollution (Liu et al., 2015a; Centi et al., 2013; Davis et al., 2010). For its renewable and environmentally friendly nature (L. Li et al., 2015; McFarland, 2014; Saboe et al., 2014), the research on solar energy storage technologies has become a hotspot of the sustainable energy field (N. Li et al., 2015; Moth-Poulsen et al., 2012). Among the multitude of storage devices (Liu et al., 2010), phase change material (PCM) (Giro-Paloma et al., 2016; Zhang et al., 2016; Xu et al., 2015) has a huge advantage for high thermal storage density via a phase transition process (C. Liu et al., 2015; Hyun et al., 2014; Ji et al., 2014; Wang et al., 2013).

In recent years, varieties of PCM were utilized for latent heat thermal energy storage (LHTES) (Alam et al., 2015; Chen et al., 2015; Chung et al., 2015; Galione et al., 2015; Liu et al., 2015b). Fatty acid as an organic solid-liquid PCM is one of the most promising materials for high energy storage capacity and small volume change during the phase change process (Cao et al., 2015; Zong et al., 2015; Behzadi and Farid, 2014). However, the application of organic PCM is limited by leakage in the melting

process, which leads to the loss of PCM and the contamination of equipment. Various supporting materials have been used for encapsulating the PCM to prevent the leakage, such as concrete (Memon et al., 2015), SiO<sub>2</sub> (Wu et al., 2015), TiO<sub>2</sub> (Cao et al., 2014), polymers (Al-Shannaq et al., 2015) and minerals (Lu et al., 2015). Among these supporting materials, porous minerals are considered to be ideal materials for practical application with the advantages of abundant natural resources, low cost and environmentally friendly nature. The common minerals for enhancing the structural and chemical stabilities of composite PCM include expanded perlite (Zhang et al., 2015), expanded graphite (Ling et al., 2015), expanded vermiculite (Chung et al., 2015; Li and Yang, 2013), kaolinite (Liu and Yang, 2014, 2015), halloysite (Liang et al., 2016), montmorillonite (Fang et al., 2008), wollastonite (Xu and Yang, 2014), etc. The traditional preparation method of PCM with minerals is mixing and impregnating the PCM into the pores of minerals. The melted PCM is trapped in the pore structure of minerals and prevented from leakage, and the amount of impregnated PCM depends on the porous features. However, the composite PCM prepared via impregnation method has limited thermal storage capacity due to the low content of phase change compounds.

Microencapsulation applied in the thermal energy storage is wrapping the PCM with shell materials, which could contain more phase change compounds compared with the impregnation method. The common shell materials are mainly polymers, such as polyethylene (Karkri et al., 2015), polymethylmethacrylate (Wang et al., 2014), and

\* Corresponding author.

\*\* Correspondence to: H. Yang, Centre for Mineral Materials, School of Minerals Processing and Bioengineering, Central South University, Changsha 410083, China.

E-mail addresses: [franch@csu.edu.cn](mailto:franch@csu.edu.cn) (L. Fu), [hmyang@csu.edu.cn](mailto:hmyang@csu.edu.cn) (H. Yang).

polycarbonate (Zhang et al., 2012), among others. However, the polymers as shell materials can release harmful components at higher operating temperatures due to their low thermal and mechanical stabilities. Montmorillonite possesses natural two-dimensional layer-like morphology with high specific surface area and thermal stability (Peng et al., 2016a, 2016b, 2016c), which may be appropriate as the shell material for encapsulating the PCM (Jacob and Bruno, 2015).

In this study, the montmorillonite/stearic acid microcapsules (Mt/SA microcapsules) containing stearic acid core with montmorillonite shell were first designed and prepared via self-assembly of Mt in the SA emulsion. The microstructure, property and reliability of the Mt/SA microcapsules were investigated. Moreover, the thermal storage and release performances of Mt/SA microcapsules were tested and compared with Mt/SA composites prepared via vacuum impregnation.

## 2. Experimental

Montmorillonite (Mt) used was unmodified Na-montmorillonite from Zhejiang, China. The main chemical compositions of Mt included (wt.%): SiO<sub>2</sub> (61.5), Al<sub>2</sub>O<sub>3</sub> (19.3), MgO (3.5), Fe<sub>2</sub>O<sub>3</sub> (1.4), Na<sub>2</sub>O (2.8), CaO (2.5), K<sub>2</sub>O (0.6) and loss on ignition (8.4). Its cation exchange capacity was 1.25 mmol/g. Stearic acid (SA, C<sub>18</sub>H<sub>36</sub>O<sub>2</sub>), hexadecyltrimethylammonium bromide (CTAB, C<sub>16</sub>H<sub>33</sub>(CH<sub>3</sub>)<sub>3</sub>NBr), tetraethoxysilane (TEOS, Si(OC<sub>2</sub>H<sub>5</sub>)<sub>4</sub>) and ammonia (NH<sub>3</sub>·H<sub>2</sub>O) were purchased from Sinopharm Chemical Reagent Co. Ltd. The Mt/SA microcapsules containing SA core with Mt shell were prepared by self-assembly of Mt in the SA emulsion. 3.00 g of SA was added to 100 mL of distilled water at 90 °C. SA was melted and the mixtures were stirred vigorously for 30 min to obtain SA emulsion. 1.00 g of Mt was added in 100 mL to distilled water using 0.10 g of CTAB as a dispersing agent with stirring for 30 min. The Mt dispersion was mixed into the SA emulsion, followed with stirring for 30 min at 90 °C. The dispersion was cooled down to ambient temperature with stirring. 1 mL of TEOS was then added with stirring for 10 min, and 0.2 mL of aqueous ammonia was dripped in the dispersion. The dispersion was filtered at 90 °C for 24 h and dried at 60 °C for 24 h to obtain the Mt/SA microcapsules.

For comparison, Mt/SA composites were obtained by absorbing SA into Mt via vacuum impregnation. 3.00 g of SA and 1.00 g of Mt were mixed in a conical flask, which was kept at 90 °C for 1 h and maintained at air pressure of −0.1 MPa. The Mt/SA composites were obtained after thermally filtered at 90 °C for 24 h and dried at 60 °C for 24 h. The amount of SA in microcapsules and composites is evaluated by weighing the final products and the leaked SA.

X-ray diffraction (XRD) analysis was performed using a DX-2700 X-ray diffractometer with Cu K $\alpha$  radiation ( $\lambda = 0.15406$  nm) at 40 kV and 40 mA. The scanning ranges were from 3° to 80° with step scan size of 0.01°, scanning speed of 0.02°/s, divergence slit of 0.5° and anti-scatter slit of 0.5°. Fourier transform infrared (FTIR) spectra analysis was performed on a Nicolet Nexus 670 FTIR spectrophotometer with KBr tablet, the sample concentration is 0.5%, and 30 scans were accumulated. The spectral ranges were between 4000 and 400 cm<sup>−1</sup> with a resolution of 2 cm<sup>−1</sup>. The optical microscope image was obtained by petrographic microscopy using a Leica DFC480 photomicroscope. The size distribution of particle was analyzed via laser diffraction method with a Malvern Mastersizer. The scanning electron microscope (SEM) image was obtained using a JEOL JSM-6360LV electron microscope at an accelerating voltage of 20 kV. The sample particles for SEM analysis were adhered on conductive adhesive and sprayed with conductive coating of Au. The SEM analysis was performed in a high vacuum mode. Differential scanning calorimetry (DSC) was conducted with a NETZSCH DSC 200 F3 Maia instrument (Selb, Germany), and the heating rate was 1 °C/min with the atmosphere of argon to avoid oxidation.

To evaluate the energy storage performance of the samples, the samples were placed in the test tube, and then it was kept at 80 °C. After the sample temperature was up to 80 °C, the natural cooling-off process was performed at ambient temperature. The temperatures of samples were

monitored every 5 s by a temperature recorder (SSN-11E), and energy storage curves were obtained from the test data.

The thermal stability of Mt/SA microcapsules was evaluated via 100 thermal cycles. Each thermal cycle comprised a melting and freezing of Mt/SA microcapsules. Mt/SA microcapsules were placed in a test tube at 90 °C to melt, and then cooled at ambient temperature to freeze. The sample after thermal cycle was analyzed through XRD, SEM, FTIR and DSC, and the error is less than 10%.

## 3. Results and discussion

The typical reflection at 1.2 nm was attributed to the (001) reflection of Na-montmorillonite (Fig. 1), which had main reflections at 19.8° and 35.1° (Cipolletti et al., 2014). The very broad basal reflection may indicate the presence of a second reflection at lower 2-theta angle possibly due to the intercalation of CTAB. The reflections at 6.8°, 21.5°, and 23.8° were ascribed to the SA with good crystalline structure (Lu et al., 2010a, 2010b). The reflections of Mt and SA all appeared in the XRD patterns of Mt/SA microcapsules and composites. The relative intensity of SA reflections in Mt/SA microcapsules was higher than that of Mt/SA composites, indicating that the SA in Mt/SA microcapsules had higher loading capacity and crystallinity. In the XRD patterns of Mt/SA microcapsules and Mt/SA composites, the reflections of Mt and SA were partly overlapped at low 2-theta angles. The basal spacing of Mt in the Mt/SA microcapsules and Mt/SA composites had no significant change, indicating that SA was hardly intercalated into the layers of Mt.

In the FTIR spectrum of Mt (Fig. 2), the bands at 471 and 1022 cm<sup>−1</sup> corresponded to the bending vibration of Si—O and the stretching vibration of O—Si—O, respectively (Liu et al., 2013). The broad band at 3453 cm<sup>−1</sup> could be attributed to the interlayer water with a variety of orientations and interactions. The —OH bending and stretching vibration were found at 1637 and 3620 cm<sup>−1</sup> (X. Li et al., 2015; Li and Yang, 2014). The broad band at 1441 cm<sup>−1</sup> and the small band at 2523 cm<sup>−1</sup> were possibly due to intercalation of the CTAB. For SA, the absorption bands at 2918 and 2849 cm<sup>−1</sup> were assigned to the C—H stretching vibrations of —CH<sub>2</sub> and —CH<sub>3</sub>, respectively. The absorption bands at 723 and 1466 cm<sup>−1</sup> came from the rocking vibration and deformation vibrations of —CH<sub>2</sub> and —CH<sub>3</sub>. The absorption band at 1703 cm<sup>−1</sup> was ascribed to C=O stretching vibrations.

In the spectrum of Mt/SA composite (Fig. 2), the bands assigned to Mt at 3629, 1029, 518 and 466 cm<sup>−1</sup>, and the bands corresponding to SA at 2917, 2850, 1704 and 1467 cm<sup>−1</sup> appeared without obvious new bands, indicating that in the Mt/SA composites just a physical

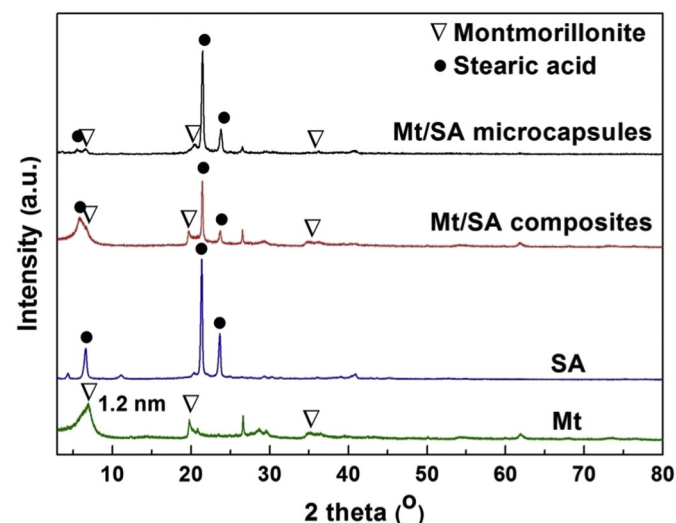


Fig. 1. XRD patterns of SA, Mt, Mt/SA microcapsules and Mt/SA composites.

Download English Version:

<https://daneshyari.com/en/article/5469067>

Download Persian Version:

<https://daneshyari.com/article/5469067>

[Daneshyari.com](https://daneshyari.com)